Microstrip Patch Antenna System With Enhanced Inter-Port Isolation for Full-Duplex/MIMO Applications

JOGESH CHANDRA DASH[ID]**, (Member, IEEE), AND DEBDEEP SARKAR**[ID]**, (Member, IEEE)**
Department of Electrical Communication Engineering, Indian Institute of Science, Bengaluru, Karnataka 560012, India
Corresponding author: Jogesh Chandra Dash (jcdash92@gmail.com)

ABSTRACT In this paper, we propose a closely spaced two-port microstrip patch antenna system with significant isolation enhancement (> 90 dB), which can be deployed for MIMO as well as full-duplex transceiver systems. We deploy a resonant combination of rectangular defected ground structure (DGS) and a near-field decoupling structure (NFDS) in the vicinity of a closely spaced (inter-element spacing $= 0.01\lambda_0$) two-port microstrip patch antenna system at 5.85 GHz. This drastically reduces the port-to-port mutual coupling (< -90 dB), which can help in self-interference cancellation for full-duplex point of view without any additional circuitry, while still preserving desired impedance matching performance (< -15 dB). The broadside gain of individual antennas in the two port MIMO system is 7.11 dBi, with 97% efficiency and co-to-cross-polar level < 25 dB. The proposed concept is validated by full-wave simulation in CST Microwave Studio, as well as experimental results on fabricated prototype. Moreover, MIMO performance metrics such as total active reflection coefficient (*TARC*), envelop correlation coefficient (*ECC*) and channel capacity loss (*CCL*) are analysed using simulation and measurement.

INDEX TERMS Full-duplex, MIMO, mutual coupling reduction, microstrip antenna, self-interference cancellation.

I. INTRODUCTION

FD (Full-duplex) antenna systems have garnered significant attention in the context of high data rate wireless communication system design, since they concurrently use same time/frequency slot for both transmission and reception, leading to enhanced spectral efficiency compared to their half-duplex (HD) counterparts [1] (See Fig. 1 for a schematic representation of HD and FD communication system). However, the FD communication system suffers from self-interference (SI) problem, that occurs due to the signal emanated by the device's own transmitter, which interferes with the received signal of interest [2]. In a broad sense, the SI cancellation approaches available in literature can be classified in two modes: *passive* and *active*, where the *active* strategy can be subdivided into analog and digital techniques [2]. *Passive* mode of SI cancellation (also known as "antenna cancellation") relies on mutual coupling reduction between the transmitter and receiver antenna in the

The associate editor coordinating the review of this manuscript and approving it for publication was Shah Nawaz Burokur[ID].

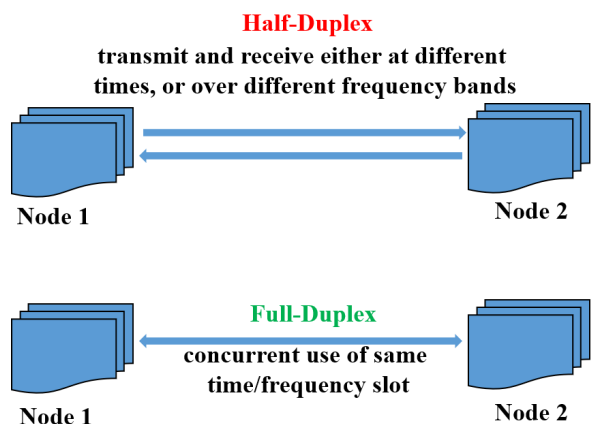FD system, while the *active* SI reduction strategies are implemented in the analog/digital base-band stages. However, analog SI cancellation cannot provide sufficient isolation to prevent the saturation of active components such as low nose amplifier (LNA) and analog-to-digital converter (ADC), prior to the digital SI cancellation [3]. Therefore, to augment the active (analog and digital) SI cancellation techniques and reduce the system cost, it is judicious to use passive antenna mutual coupling (MC) reduction techniques in FD antenna systems. Apart from the FD technology, MIMO (multiple-input multiple-output) antenna system is another enabling technology for the advanced 4G/5G wireless communication that provided high data rate and enhanced spectral efficiency. However, MIMO antenna systems also require low inter-port mutual coupling to cater optimum performance.

It should be noted that, MIMO antenna systems can operate with port-to-port MC level of -15 dB. For example, a three-element diversity MIMO antenna with MC less than -15 dB is presented in [4]. MC less than -20 dB between two microstrip MIMO antenna using an inverted fork shaped decoupling structure (IFSD) is presented in [5].

FIGURE 1. Schematic representation of HD and FD wireless communication systems.

FIGURE 2. Schematic diagram of proposed two-port antenna at 5.85 GHz.

has not been reported in the FD antenna systems of open literature. Moreover, the proposed design is suitable for upper WLAN and 5G NR-U band [30] MIMO application.

II. PROPOSED TWO-PORT ANTENNA DESIGN

The proposed two-port antenna comprises of a three-layer structure as shown in Fig. 2. The co-axially fed microstrip patch antenna in Fig. 3(a) is designed on a RTD5880 substrate of 1.57 mm thickness, having $\varepsilon_r = 2.2$ and $\tan \delta = 0.0009$. An inverted L-shaped structure is connected from one end of the patch radiating edge and directed toward the non-radiating edge to create an asymmetry in the design, thereby reducing the inter-element H-plane coupling. A rectangular portion having dimension of $l_d \times w_d$ is etched from the ground plane to design a defected ground structure (DGS) (Fig. 3(b)). Another dielectric sheet RT5880LZ of 0.5 mm thickness having $\varepsilon_r = 1.96$ and $\tan \delta = 0.0019$ is placed above the microstrip antenna at h_2 height (Fig. 3 (c-d)). Inspired by the antenna decoupling surface proposed in [26], two parallel microstrip lines are designed on that dielectric sheet immediately above the inter-element spacing and the near field region, which act as NFDS. Note that the NFDS substrate should be low loss and its dielectric permittivity should be as low as possible to avoid the effect of dielectric loading on the antenna radiation performance. The resonant combination of DGS and the NFDS helps in reducing field coupling between the two nearby antennas.

A detailed analysis of aforementioned decoupling mechanism by examining the field distribution has been provided in the subsequent section. It has been shown that the reduction of field coupling, both E and H field, helps in reducing the mutual coupling between the nearby radiating elements to an extremely low value.

III. EXPLANATION OF DECOUPLING MECHANISM IN PROPOSED TWO-PORT ANTENNA

In this section, we present the design evolution of the proposed two-port antenna along with its decoupling mechanism. For each design stage, we examine the field distribution, mutual coupling (S_{21}/S_{12}) and impedance matching (S_{11}) levels and the 2D radiation pattern.

- *Stage-0:* Initially, an antenna system having two closely spaced ($g_2 = 0.06\lambda_0$) microstrip patches (dimensions of $l_1 \times w_1$ each) are designed (Fig. 4). The patch antenna works at 5.85 GHz LTE band with good impedance

Similarly, several techniques for MIMO antenna systems are available in literature, which result in reduced MC levels around -15 dB, utilizing defected ground structures (DGS) [6] – [8], split-ring resonators (SRR) [9], metamaterial based isolator [10], modified U-shaped microstrip resonators, meander-lines, EBG structures, parallel-coupled line resonators (PCR), frequency selective surface (FSS), slot and using pixelization and binary optimization (PBO) were proposed in [11]–[13] and [14]–[17] and [18] respectively. Moreover, a review on MC and its reduction techniques for other MIMO system are provided in [19] and [20] respectively.

However, FD antenna systems demand far greater degree of MC reduction (< -60 dB) [21]. A passive SI reduction of about 60 dB is obtained for three element FD antenna system is provided in [21]. Antenna cancellation of more than 35 dB is achieved in [22] using 180^0 hybrid and a DGS structure. A pattern/polarization diversity FD antenna system having antenna cancellation of more than 30 dB is presented in [23]. But these FD antenna systems have large inter-element separation, which is not suitable for compact systems. A reconfigurable polarization-based antenna cancellation (PAC) technique is provided in [24] to achieve more than 50 dB antenna cancellation in the expense of antenna design and fabrication complexity. Moreover, it is mentioned in [20] that to decode the signal from received antenna for a 802.15.4 FD system, 60 dB SI reduction is desired using antenna cancellation method (to combat ≈ -100 dB system noise floor). Therefore, for smooth functioning of Tx and Rx module for a FD application, the passive SI cancellation at electromagnetic level should be at least 60 dB.

In this paper, we propose a MC reduction technique in a closely spaced two-port patch antenna system for FD as well as MIMO application. The proposed technique uses antenna design asymmetry with the resonant combination of DGS and near-field decoupling structure (NFDS). To the best of the authors' knowledge, isolation enhancement of > 90 dB with inter-element spacing $< 0.01\lambda$ and compact antenna volume,
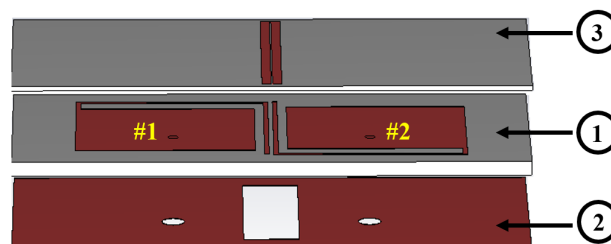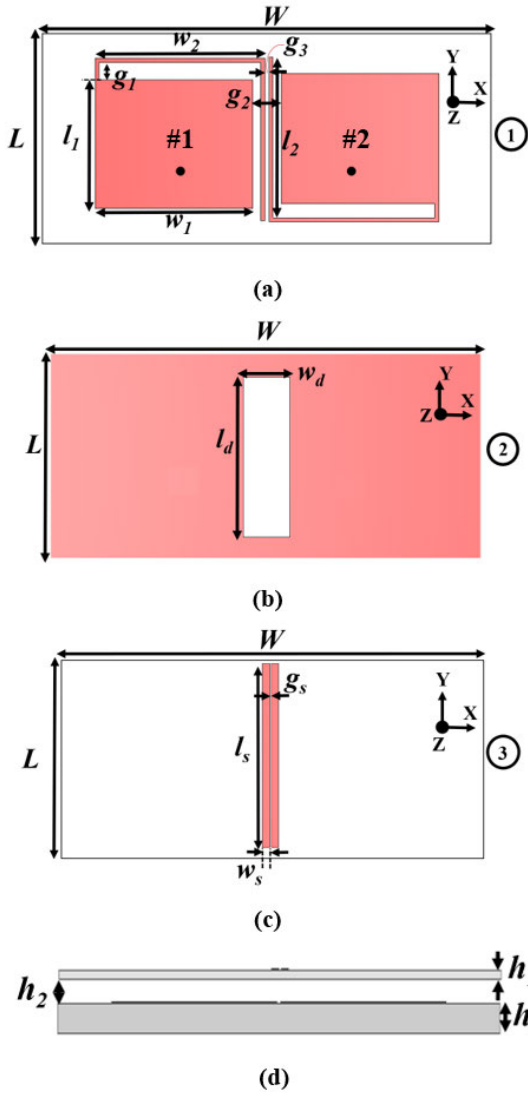
(a)

(b)

(c)

(d)

FIGURE 3. Proposed two-port antenna showing dimensions for individual layers in Fig. 1: (a) top layer, (b) middle layer, (c) ground plane, (d) side view. Dimensions: $L = 1.092\lambda_0$, $W = 0.507\lambda_0$, $l_1 = 0.31\lambda_0$, $w_1 = 0.38\lambda_0$, $l_2 = \lambda_0$, $w_2 = 0.4\lambda_0$, $g_1 = 0.039\lambda_0$, $g_2 = 0.068\lambda_0$, $g_3 \approx 0.01\lambda_0$, $l_d = 0.394\lambda_0$, $w_d = 0.117\lambda_0$, $l_s = 0.478\lambda_0$, $w_s = 0.018\lambda_0$, $g_s = 0.00429\lambda_0$, $h_1 = 0.0057\lambda_0$, $h_2 = 0.0136\lambda_0$, $h_3 = 0.03\lambda_0$.

matching ($|S_{11}| < -10$ dB). However, strong H- and E-field coupling between the nearby antennas ($|S_{21}| = |S_{12}|$ about -11 dB) can be observed (Fig. 5). The 2D radiation patterns (E/H plane) of antenna #1 and #2 at stage-0 are shown in Fig.6(a) and (b) respectively. The patterns show the good cross polar level (below -20 dB) at both E and H plane for two antenna elements.

- *Stage-1*: Next, the L-shaped structure of Fig. 3(a) is included to create an asymmetry in the microstrip antenna structure designed in stage 0 to reduce the mutual coupling (Fig. 7), which can be verified from the H-field distribution in Fig. 7. As compared to stage-0, stage-1 exhibits 8 dB increase in the isolation. The L-shaped structure increases the effective electrical length of individual antenna elements, causing a shift
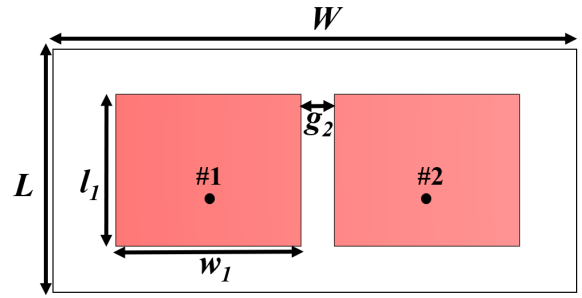
FIGURE 4. Schematic of the proposed two-port antenna at stage 0 (only top layer with two side-by-side microstrip patches is shown).
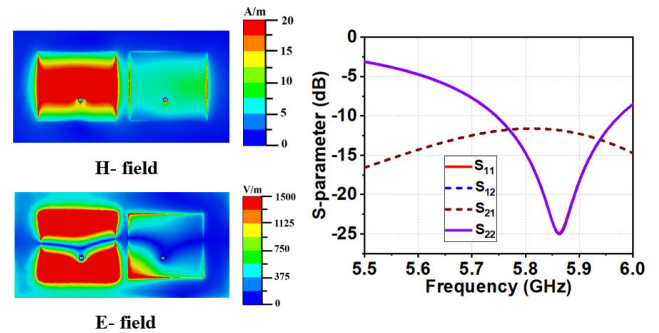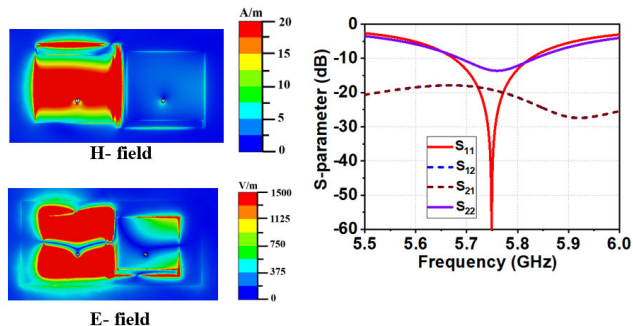

FIGURE 5. H and E field distribution on the patches of the stage-0 antenna configuration at 5.85 GHz, along with the frequency variation of S-parameters (Port 1 is excited, while keeping port 2 terminated with matched load).Note that, we have $S_{11} = S_{22}$ due to structural symmetry (reciprocity ensures $S_{12} = S_{21}$).
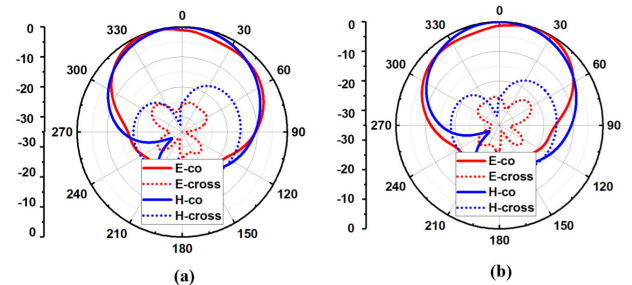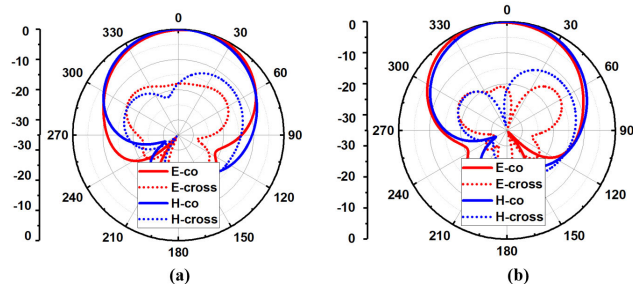

FIGURE 6. Simulated 2D radiation pattern at 5.85 GHz of antenna design stage 0 (Fig. 4): (a) Antenna #1, (b) Antenna #2.

in the operating frequency from 5.85 GHz at stage-0 to 5.75 GHz at stage-1. However, the asymmetry in the antenna design varies the individual antenna impedance matching and the E-field coupling still exist as shown in Fig. 7. The 2D radiation pattern for the stage-1 antenna configuration is shown in Fig. 8. The asymmetry introduced in this stage increases the cross-polar level than the antenna configuration at stage-0. However, the cross polar level is below -15 dB at the broadside direction for both the antenna elements(see Fig. 8).

- *Stage-2*: The stage-2 incorporates both the DGS (Fig. 3(b)) and the NFDS (Fig. 3(c)) in conjunction with the asymmetric patch configuration of stage-1. DGS loading in the ground plane reduces the surface wave

FIGURE 7. H and E field distribution on the patches of the stage-1 antenna configuration (see only Fig. 3(a)) at 5.85 GHz, along with the frequency variation of S-parameters (Port 1 is excited, while keeping port 2 terminated with matched load). Note that, due to structural asymmetry, we have $S_{11} \neq S_{22}$ (reciprocity ensures $S_{12} = S_{21}$, as expected).


FIGURE 8. Simulated 2D radiation pattern at 5.7 GHz of antenna design stage 1 (Fig. 3(a)): (a) Antenna #1, (b) Antenna #2.

excitation thereby improving the cross-polar response (see Fig. 14) and the dimension of the DGS determines stop band effect by incorporating transmission zero at the frequency of interest [27], [28]. The height between NFDS and the antenna ground plane determines the phase of the partially diffracted wave to cancel out the coupled wave. Also, height between defected ground and NFDS such ensures extremely low value of the inter-element mutual coupling. The dimensions of DGS and NFDS as well as the height between them is carefully decided using parametric analysis as shown in Fig. 9.

The parametric study is conducted for the DGS design parameters l_d and w_d and the NFDS design parameters l_s, w_s and h_2. It is observed that the variation of l_d and w_d have very less impact on impedance matching, however these decide the resonant frequency for S_{21} (S_{12}). As shown in Fig. 9 (a) and (b), there is a gradual decrease (increase) in the frequency for mutual coupling parameter with gradual increase (decrease) in l_d (wd) values is observed. On the other hand, the variation of NFDS design parameters (l_s, w_s and h_2) alter the antenna operating frequency due the superstate loading effect. Moreover, the NFDS design parameters improve the mutual coupling performance at the frequency of interest as shown in Fig. 9 (c-e). The parametric study provides an intuition for NFDS design in the presence of DGS to reduce the mutual coupling. Moreover, the study
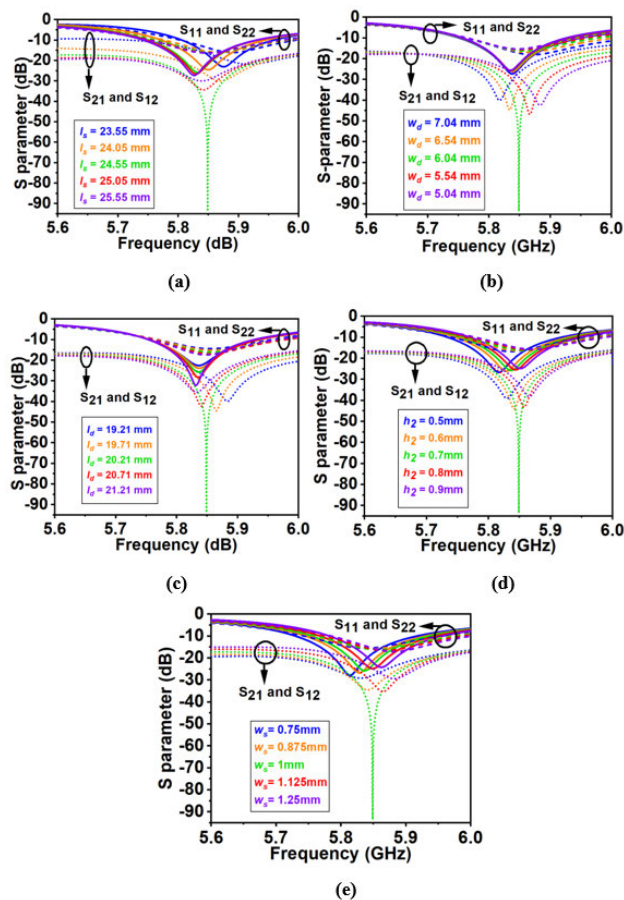

FIGURE 9. Studies on parameters: (a) l_d, (b) w_d, (c) l_s, (d) w_s, (e) h_2, to understand the respective effects on S-parameter response of the proposed two-port antenna configuration.
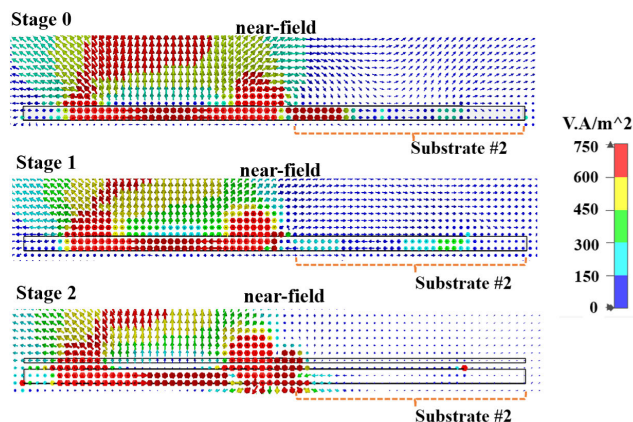
FIGURE 10. Study of power flow between the antenna elements in the near-field region and inside the substrate for different stages of antenna design (Port 1 is excited, while keeping port 2 terminated to the matched load).

of power flow between the antenna elements for different stages of antenna design is provided in Fig. 10. As stage-0 (Fig. 4), as the antenna elements are very closely spaced having no decoupling technique is being used the power flow between the antenna elements through substrate and the near-field region is very high (see Fig. 10). The asymmetry
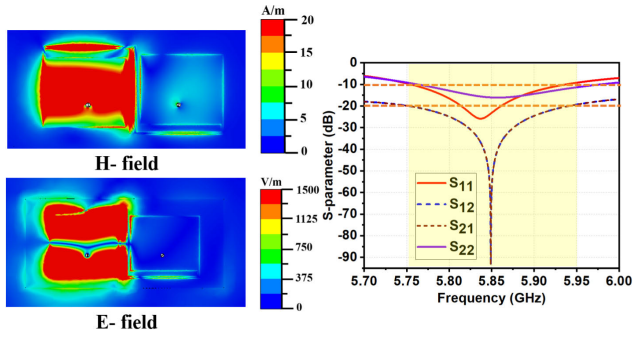
FIGURE 11. H and E field distribution on the patches of the stage-2 antenna configuration (see complete Fig. 3) at 5.85 GHz, along with the frequency variation of S-parameters (Port 1 is excited, while keeping port 2 terminated with matched load). Here also due to structural asymmetry, we have $S_{11} \neq S_{22}$ (reciprocity ensures $S_{12} = S_{21}$, as expected).
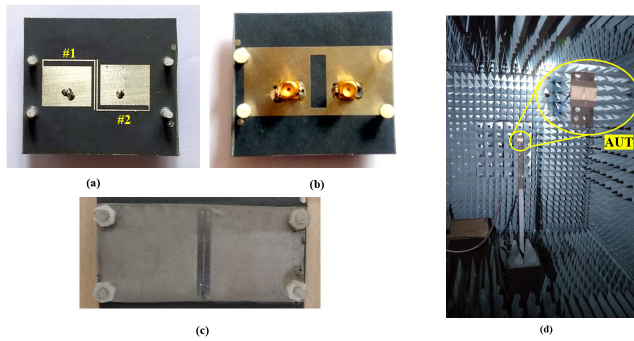

FIGURE 12. Fabricated proposed antenna prototype: (a) Top-view (without superstrate), (b) Bottom-view, (c) Top-view (with superstrate), (d) Far-field radiation pattern measurement setup in Anechoic chamber.

introduced at the stage-1 (Fig. 3(a)) antenna design reduces the power flow in the substrate region, from antenna #1 to antenna #2, compared to stage-0 (see Fig. 10). At stage-2 the use of DGS and NFDS along with the asymmetry introduced in stage-1 completely prevent the power flow both in the substrate region and near-filed region of antenna #2 from antenna #1(see Fig. 10).

The combined resonant effect of DGS and NFDS reduces both the H-field and E- field coupling between the nearby antenna as shown in Fig. 11. Consequently, the proposed technique exhibits the good impedance matching at 5.85 GHz desired operating frequency and reduces the mutual between the nearby antennas having $S_{11} < -10$ dB and $S_{21}/S_{12} < -90$ dB respectively as shown in Fig. 11. Antenna #1 covers 5749 MHz-5949 MHz operating band having -10 dB impedance bandwidth of 200 MHz, while antenna #2 covers 5762 MHz- 5978 MHz operating band having -10 dB impedance bandwidth 216 MHz. The overlapping bandwidth of the antenna is 187 MHz.

IV. PROTOTYPE FABRICATION AND MEASUREMENT RESULTS

Fig. 12(a-c) depicts the fabricated antenna prototype. The superstrate with NFDS structure is supported and height h_2 is adjusted by four dielectric screws at four corners of the
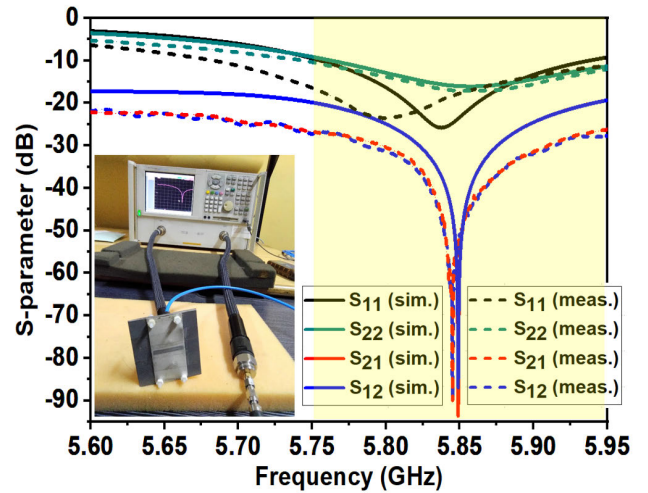
FIGURE 13. Frequency variation of simulated and measured S-parameters for the proposed antenna in Fig. 1.
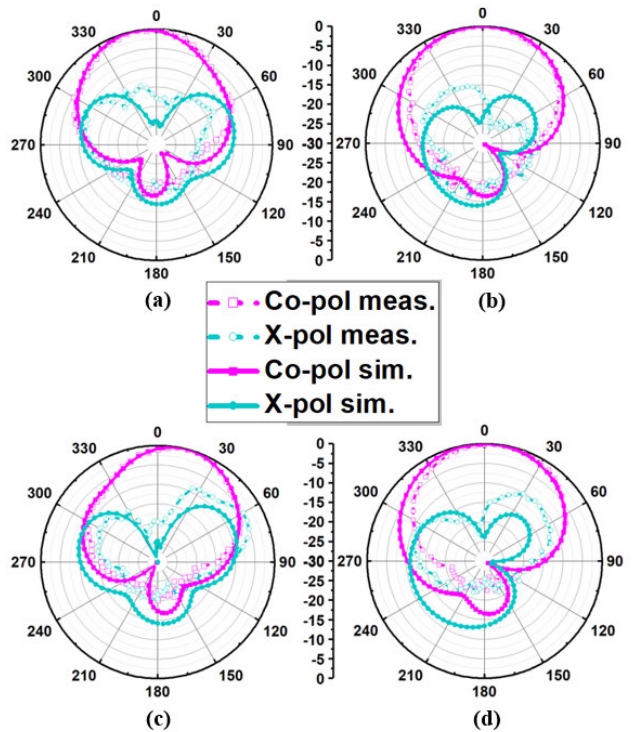
FIGURE 14. Simulated and measured patterns at 5.85 GHz: (a) E-plane (antenna 1), (b) H-plane (antenna 1), (c) E-plane (antenna 2), (d) H-plane (antenna 2).

antenna (see Fig. 13). The S-parameters for the proposed two-port antenna are measured using Agilent N5230A PNA and compared with the simulation results (see Fig. 13). The measured inter-element isolation at operating frequency is $\approx$ 90 dB and it is more than 25 dB over the complete operating band. The deviation in the S-parameter is due to the fabrication tolerances and surrounding effects. Fig. 12(d) depicts the antenna far-field measurement setup. The measured and simulated far-field E-plane and H-plane co/cross polar pattern in provided in Fig. 14. The proposed
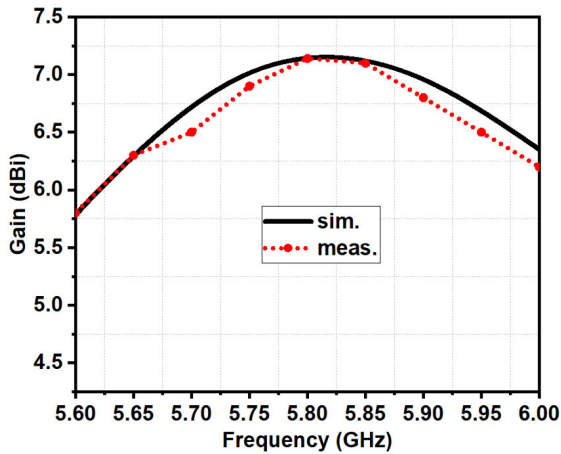
FIGURE 15. Frequency variation of simulated and measured gain for the proposed antenna.

TABLE 1. Comparison of proposed two-port antenna with other structures available in open literature.

Ref.	edge spacing (λ_0)	OF (GHz)	IBW (%)	Isolation (dB)	Decoupling Technique	max. Gain (dBi)
[6]	0.06	2.45	1.5	>25	Ring DGS	NA
[10]	0.135	5.8	NA	>24.5	Metamaterial structure	4
[11]	0.1	5.4	NA	>23	Modified-U shape DS	4.24
[12]	0.11	4.8	5.21	>16	SMLR	NA
[15]	0.07	3.5	2.8	>35	PCR	~6
[16]	0.13	5.25	2.6	>16	FSS	9
[17]	0.19	10	3	>37	Slot	
[18]	0.14	4	NA	>45	PBO	5.3
[22]	NA	2.4	9	>35	180 hybrid/ DGS	4
[24]	0.09	4.7	6.5	>50	PAC	~3
Prop.	≈ **0.01**	**5.85**	**3.41**	**>90**	**Asymmetry +DGS+NFDS**	**7.11**

(OF: operating frequency, IBW: 10dB impedance bandwidth)

antenna exhibits a maximum gain of 7.11 dBi at 10° broadside tilt angle and 6.69 dBi gain at 0° broadside direction. The simulated and measured gain over frequency curve is provided in Fig. 15.

A comparison study of these earlier published work with proposed technique is provided in Table 1. The comparison study shows that the proposed technique exhibits maximum possible isolation (> 90 dB) with very close inter-element spacing (≈ $0.01\lambda_0$) compared to the earlier published works. Moreover, the impedance bandwidth and gain of the proposed antenna are comparable with the earlier reported results as provided in Table-1.

A. MIMO PERFORMANCE PARAMETERS

MIMO performance study of the proposed two-port antenna configuration is carried out by computing total active reflection coefficient (*TARC*), envelop correlation coefficient (*ECC*) and channel capacity loss (*CCL*) in the operating band (see Fig. 16). The relevant mathematical formulations for *ECC*, *CCL* and *TARC* are provided in [4]. The value of *ECC* is much less than 0.5 in the uniform propagation environment,
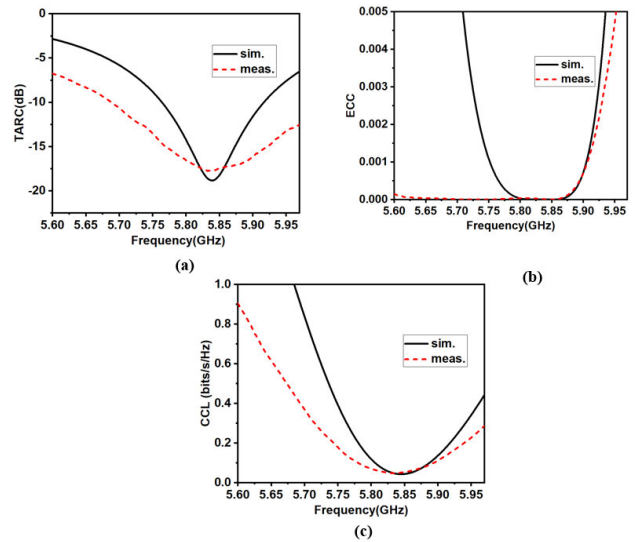

FIGURE 16. Frequency variation of MIMO performance metrics for the proposed two-port antenna system: (a) *TARC*, (b) *ECC*, and (c) *CCL*.

which indicates excellent diversity performance, which is further reflected in the low value of channel capacity loss (< 0.5 bits/s/Hz) in the operating band. Also, the *TARC* being less than −10 dB around 5.85 GHz indicates that the two port system is capable of operating efficiently in "active" (simultaneous port-excitation) condition.

V. CONCLUSION

In this brief, a closely spaced microstrip antenna configuration with good impedance matching ($|S_{11}| < −15$ dB), very high inter-port isolation (> 90 dB), individual antenna gain > 7 dBi and radiation efficiency of 97% (antenna total efficeicny:96.9%) is presented for FD and MIMO applications at 5.85 GHz (upper WLAN frequencies [29] and 5G NR-U band [30]). The relevant design steps are systematically described, with emphasis on E/H-field coupling and S-parameter analysis with parametric variation. The proposed design concept is very generic (i.e. can be scaled to any other frequency range), and are validated through prototype fabrication and experimental measurements of S-parameters, radiation patterns (2D cuts) and post processed MIMO performance metrics (*ECC*, *TARC* and *CCL*). Table-1 clearly demonstrates that the best performance is achieved in terms of high inter-port isolation for very small edge-to-edge antenna spacing, without compromising much on the gain and impedance bandwidth. Therefore the proposed microstrip antenna system is an excellent candidate for FD and MIMO applications, where self-interference cancellation through analog mode and inter-port isolation are key desired attributes respectively.

ACKNOWLEDGMENT

REFERENCES

[1] A. Sabharwal, P. Schniter, D. Guo, D. W. Bliss, S. Rangarajan, and R. Wichman, "In-band full-duplex wireless: Challenges and opportunities," *IEEE J. Sel. Areas Commun.*, vol. 32, no. 9, pp. 1637–1652, Sep. 2014.

[2] K. Gbafa, A. Diallol, P. L. Thuc, and R. Staraj, "Tx/Rx antenna system for full-duplex application," in *Proc. IEEE Int. Symp. Antennas Propag. USNC/URSI Nat. Radio Sci. Meeting*, Boston, MA, USA, Jul. 2018, pp. 1571–1572.

[3] A. Batgerel and S. Y. Eom, "High-isolation microstrip patch array antenna for single channel full duplex communications," *IET Microw., Antennas Propag.*, vol. 9, no. 11, pp. 1113–1119, Aug. 2015.

[4] Y. Sharma, D. Sarkar, K. Saurav, and K. Srivastava, "Three-element MIMO antenna system with pattern and polarization diversity for WLAN applications," *IEEE Antennas Wireless Propag. Lett.*, vol. 16, pp. 1163–1166, 2017.

[5] J. C. Dash, N. Kalva, S. Kharche, and J. Mukherjee, "Isolation enhancement of closely spaced MIMO system using inverted fork shaped decoupling structure," in *Proc. 14th Eur. Conf. Antennas Propag. (EuCAP)*, Copenhagen, Denmark, Mar. 2020, pp. 1–3.

[6] R. Anitha, V. P. Sarin, P. Mohanan, and K. Vasudevan, "Enhanced isolation with defected ground structure in MIMO antenna," *Electron. Lett.*, vol. 50, no. 24, pp. 1784–1786, 2014.

[7] H. Xing, X. Wang, Z. Gao, X. An, H.-X. Zheng, M. Wang, and E. Li, "Efficient isolation of an MIMO antenna using defected ground structure," *Electronics*, vol. 9, no. 8, p. 1265, Aug. 2020.

[8] Z. Niu, H. Zhang, Q. Chen, and T. Zhong, "Isolation enhancement for 1×3 closely spaced E-plane patch antenna array using defect ground structure and metal-vias," *IEEE Access*, vol. 7, pp. 119375–119383, 2019.

[9] D. Sarkar and K. V. Srivastava, "A compact two-port MIMO antenna with enhanced isolation using SRR-loaded slot-loop," in *Proc. IEEE Appl. Electromagn. Conf. (AEMC)*, Aurangabad, India, Dec. 2017, pp. 1–2.

[10] A. Iqbal, O. A. Saraereh, A. Bouazizi, and A. Basir, "Metamaterial-based highly isolated MIMO antenna for portable wireless applications," *Electronics*, vol. 7, no. 10, p. 267, 2018.

[11] A. Iqbal, A. Altaf, M. Abdullah, and M. Alibakhshikenar, "Modified U-shaped resonator as decoupling structure in MIMO antenna," *Electronics*, vol. 9, no. 8, p. 1321, 2020.

[12] M. G. Alsath, M. Kanagasabai, and B. Balasubramanian, "Implementation of slotted meander-line resonators for isolation enhancement in microstrip patch antenna arrays," *IEEE Antennas Wireless Propag. Lett.*, vol. 12, pp. 15–18, 2013.

[13] M. Alibakhshikenari, M. Khalily, B. S. Virdee, C. H. See, R. Abd-Alhameed, and E. Limiti, "Mutual coupling suppression between two closely placed microstrip patches using EM-bandgap metamaterial fractal loading," *IEEE Access*, vol. 7, pp. 23606–23614, 2019.

[14] M. Alibakhshikenari, M. Khalily, B. S. Virdee, C. H. See, R. A. Abd-Alhameed, and E. Limiti, "Mutual-coupling isolation using embedded metamaterial EM bandgap decoupling slab for densely packed array antennas," *IEEE Access*, vol. 7, pp. 51827–51840, 2019.

[15] K. S. Vishvaksenan, K. Mithra, R. Kalaiarasan, and K. S. Raj, "Mutual coupling reduction in microstrip patch antenna arrays using parallel coupled-line resonators," *IEEE Antennas Wireless Propag. Lett.*, vol. 16, pp. 2146–2149, 2017.

[16] T. Hassan, M. U. Khan, H. Attia, and M. S. Sharawi, "An FSS based correlation reduction technique for MIMO antennas," *IEEE Trans. Antennas Propag.*, vol. 66, no. 9, pp. 4900–4905, Sep. 2018.

[17] M. Kiani-Kharaji, H. R. Hassani, and S. Mohammad-Ali-Nezhad, "Wide scan phased array patch antenna with mutual coupling reduction," *IET Microw., Antennas Propag.*, vol. 12, no. 12, pp. 1932–1938, Oct. 2018.

[18] A. Ghadimi, V. Nayyeri, M. Khanjarian, M. Soleimani, and O. M. Ramahi, "A systematic approach for mutual coupling reduction between microstrip antennas using pixelization and binary optimization," *IEEE Antennas Wireless Propag. Lett.*, vol. 19, no. 12, pp. 2048–2052, Dec. 2020.

[19] X. Chen, S. Zhang, and Q. Li, "A review of mutual coupling in MIMO systems," *IEEE Access*, vol. 6, pp. 24706–24719, 2018.

[20] I. Nadeem and D.-Y. Choi, "Study on mutual coupling reduction technique for MIMO antennas," *IEEE Access*, vol. 7, pp. 563–586, 2019.

[21] J. I. Choi, M. Jain, K. Srinivasan, P. Levis, and S. Katti, "Achieving single channel, full duplex wireless communication," in *Proc. 16th Annu. Int. Conf. Mobile Comput. Netw. (MobiCom)*, 2010, pp. 1–12.

[22] G. Makar, N. Tran, and T. Karacolak, "A high-isolation monopole array with ring hybrid feeding structure for in-band full-duplex systems," *IEEE Antennas Wireless Propag. Lett.*, vol. 16, pp. 356–359, 2017.

[23] K. Gbafa, A. Diallo, P. Le Thuc, and R. Staraj, "High isolated MIMO antenna system for full-duplex 5G applications," in *Proc. IEEE Conf. Antenna Meas. Appl. (CAMA)*, Bali, Indonesia, Oct. 2019, pp. 49–52.

[24] J. Zhou, N. Reiskarimian, and J. Diakonikolas, "Integrated full duplex radios," *IEEE Commun. Mag.*, vol. 55, no. 4, pp. 142–151, Apr. 2017.

[25] M. Jain, J. I. Choi, T. Kim, D. Bharadia, and S. Seth, "Practical, real-time, full duplex wireless," in *Proc. ACM MOBICOM*, Las Vegas, NV, USA, 2011, pp. 301–312.

[26] K.-L. Wu, C. Wei, X. Mei, and Z.-Y. Zhang, "Array-antenna decoupling surface," *IEEE Trans. Antennas Propag.*, vol. 65, no. 12, pp. 6728–6738, Dec. 2017.

[27] J. C. Dash, G. P. Mishra, and B. B. Mangaraj, "Design of dual band patch antenna with bandwidth enhancement using complementary defected ground structure," in *Proc. 2nd Int. Conf. Contemp. Comput. Informat. (IC3I)*, Dec. 2016, pp. 271–274.

[28] I. Bahl, *Microstrip Lines and Slotlines*, 3rd ed. Norwood, MA, USA: Artech House, 2013.

[29] X. L. Sun, L. Liu, S. W. Cheung, and T. I. Yuk, "Dual-band antenna with compact radiator for 2.4/5.2/5.8 GHz WLAN applications," *IEEE Trans. Antennas Propag.*, vol. 60, no. 12, pp. 5924–5931, Dec. 2012.

[30] M. Hirzallah, M. Krunz, B. Kecicioglu, and B. Hamzeh, "5G new radio unlicensed: Challenges and evaluation," *IEEE Trans. Cognit. Commun. Netw.*, vol. 7, no. 3, pp. 689–701, Sep. 2021.

JOGESH CHANDRA DASH (Member, IEEE) received the M.Tech. degree in electronics and tele-communication engineering with RF and microwave specialization from VSSUT (formerly UCE), Burla, in 2016, and the Ph.D. degree in electrical engineering with specialization in communication and signal processing: (RF and microwave) (EE1) from the Indian Institute of Technology (IIT), Bombay, in 2021. He is currently working as a Postdoctoral Research Associate at the iDARE Laboratory, Department of Electrical Communication Engineering, Indian Institute of Science (IISc), Bengaluru. He serves as a Reviewer for several journals, such as the IEEE TRANSACTIONS ON INDUSTRIAL ELECTRONICS, IEEE ACCESS, *IET Microwave and Antenna Propagation*, and *International Journal of RF and Computer-Aided Engineering* (Wiley).

DEBDEEP SARKAR (Member, IEEE) received the B.E. degree in ETCE from Jadavpur University, in 2011, and the M.Tech. and Ph.D. degrees from the Indian Institute of Technology, Kanpur, in 2013 and 2018, respectively.

He worked as a Visiting Researcher and a Postdoctoral Fellow with the Royal Military College, Canada, from May 2017 to August 2017, and from November 2018 to February 2020, respectively. He is currently an Assistant Professor with the Department of Electrical Communication Engineering (ECE), Indian Institute of Science (IISc), Bengaluru. He has authored/coauthored more than 30 peer-reviewed journal articles so far.

Dr. Sarkar is also an IEEE Antennas and Propagation Society Young Professionals (YP) Committee Member. He was a recipient of the URSI Young Scientist Award (YSA) twice (in the APRASC 2019 and URSIGASS 2020), along with best paper awards and grants from several conferences. He has also been selected for the prestigious position of 'Infosys Young Investigator', by Infosys Foundation, Bengaluru. He is the Vice-Chair with the IEEE YP Affinity Group, Bengaluru Section. He serves as a Reviewer for several prestigious journals, such as the IEEE TRANSACTIONS ON ANTENNAS AND PROPAGATION, the IEEE TRANSACTIONS ON MICROWAVE THEORY AND TECHNIQUES, the IEEE TRANSACTIONS ON VEHICULAR TECHNOLOGY, the IEEE ANTENNAS AND WIRELESS PROPAGATION LETTERS, and *IEEE Antennas and Propagation Magazine*. He is also serving as an Associate Editor for IEEE ACCESS and *IET Microwaves, Antennas and Propagation*.